RADIATION FROM OPEN-ENDED FLANGED WAVEGUIDE WITH DIELECTRIC LOADING *

V.V. Vorobev, S.N. Galyamin†, A.A. Grigoreva, A.V. Tyukhtin
St. Petersburg State University, 7/9 Universitetskaya nab., St. Petersburg, 199034 Russia

Abstract

Terahertz radiation is considered as a promising tool for a number of applications. One of the possible ways to emit THz waves is to pass short electron bunch through a waveguide structure loaded with dielectric [1]. Previously we considered the extraction of radiation from the open end of the waveguide with dielectric loading in both approximate and rigorous formulation [2]. We also developed a rigorous approach based on mode-matching technique and modified residue-calculus technique for the case when the waveguide with dielectric is co-axial with infinite waveguide with greater radius [3]. The study presented here is devoted to the case when the waveguide with open end has a flange and enclosed into another waveguide with a greater radius. The case of the flanged waveguide in the unbounded vacuum space can be described as the limiting case of the problem under consideration. We perform analytical calculation (based on mode-matching technique and modified residue-calculus technique) for the case of vacuum waveguide with a flange (dielectric with very high permittivity instead of flange is also considered), direct numerical simulation for this case and compare results. The case of inner waveguide with flange and dielectric filling is investigated numerically.

ANALYTICAL RESULTS

In this report, we consider 3 problems (Fig. 1). In problem (a), a semi-infinite ideally conducting ($\sigma = \infty$) cylindrical waveguide with radius b enclosed into a concentric infinite waveguide with radius $a > b$. Coaxial domain (2) is filled with a homogeneous dielectric ($\varepsilon_0 > 1$). In problem (b), coaxial part is terminated by ideally conducting flange. Problem (c) differs from (b) by filling the inner waveguide with dielectric ($\varepsilon > 1$). All structures are excited by a single TM_{0l} mode propagating from the inner waveguide. Below we present rigorous theory for the problem (a), which can be easily modified for problem (b). Problem (c) is investigated numerically. Incident field in cylindrical frame ρ, ϕ, z is

$$H_{\omega\phi}^{(i)} = J_1(\rho j_{0l}/b)e^{-\gamma_{zl}^{(1)}z}, \qquad (1)$$

where $J_0(j_{0l}) = 0$, $\gamma_{zl}^{(1)} = \sqrt{j_{0l}^2 b^{-2} - k_0^2}$, $\mathrm{Re}\gamma_{zl}^{(1)} > 0$, $k_0 = \omega/c$. The reflected field in the domain (1) is

$$H_{\omega\phi}^{(1)} = \sum_{m=1}^{\infty} B_m J_0(\rho j_{0m}/b)e^{\gamma_{zm}^{(1)}z}. \qquad (2)$$

* Work supported by Russian Foundation for Basic Research (grant No. 15-02-03913) and Government of Saint Petersburg.
† s.galyamin@spbu.ru

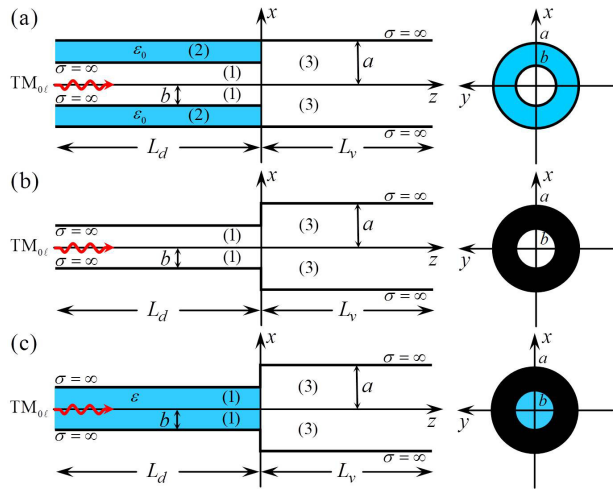

Figure 1: Geometry of the problems.

Fields generated in domains (2) and (3) are:

$$H_{\omega\phi}^{(3)} = \sum_{m=1}^{\infty} A_m J_0(\rho j_{0m}/a)e^{-\gamma_{zm}^{(3)}z}, \qquad (3)$$

$$H_{\omega\phi}^{(2)} = C_0\rho^{-1}e^{\kappa_{z0}^{(2)}z} + \sum_{m=1}^{\infty} C_m Z_m(\rho\chi_m)e^{\kappa_{zm}^{(2)}z}, \qquad (4)$$

where $\gamma_{zm}^{(3)} = \sqrt{j_{0m}^2 a^{-2} - k_0^2}$, $\kappa_{z0}^{(2)} = -ik_0\sqrt{\varepsilon_0}$, $\kappa_{zm}^{(2)} = \sqrt{\chi_m^2 - k_0^2\varepsilon_0}$, $\mathrm{Re}\gamma_{zm}^{(3)} > 0$, $\mathrm{Re}\kappa_{zm}^{(2)} > 0$,

$$Z_m(\xi) = J_1(\xi) - N_1(\xi)J_0(a\chi_m)N_0^{-1}(a\chi_m), \qquad (5)$$

χ_m is solution of dispersion relation for domain (2),

$$J_0(b\chi_m)N_0(a\chi_m) - J_0(a\chi_m)N_0(b\chi_m) = 0. \qquad (6)$$

Performing matching of $H_{\omega\phi}$ and $E_{\omega\rho} = c(i\omega\varepsilon)^{-1}\partial H_{\omega\phi}/\partial z$ for $z = 0$, and integrating separately over $0 < \rho < b$ and $b < \rho < a$ with eigenfunction of domains (1) and (2) correspondingly, we can obtain the following infinite systems for unknown coefficients:

$$\sum_{m=1}^{\infty}\left(\frac{\tilde{A}_m}{\gamma_{zm}^{(3)} - \gamma_{zn}^{(2)}} + \frac{\tilde{A}_m q_n}{\gamma_{zm}^{(3)} + \gamma_{zn}^{(2)}}\right) = 0, \qquad (7)$$

$$\sum_{m=1}^{\infty}\left(\frac{\tilde{A}_m q_n}{\gamma_{zm}^{(3)} - \gamma_{zn}^{(2)}} + \frac{\tilde{A}_m}{\gamma_{zm}^{(3)} + \gamma_{zn}^{(2)}}\right) = \frac{-4\tilde{C}_n\gamma_{zn}^{(2)}\kappa_{zn}^{(2)}}{\kappa_{zn}^{(2)} + \varepsilon_0\gamma_{zn}^{(1)}}, \qquad (8)$$

$$\sum_{m=1}^{\infty}\frac{\tilde{A}_m}{\gamma_{zm}^{(3)} - \gamma_{zp}^{(1)}} = -\delta_{lp}bJ_1(j_{0p})\gamma_{zl}^{(1)}, \qquad (9)$$

ISBN 978-3-95450-181-6

$$\sum_{m=1}^{\infty}\frac{\tilde{A}_m}{\gamma_{zm}^{(3)}+\gamma_{zp}^{(1)}}=2\tilde{B}_p\gamma_{zp}^{(1)}, \quad (10)$$

$\gamma_{z0}^{(2)}=-ik_0$, $\gamma_{zp}^{(2)}=\sqrt{\chi_m^2-k_0^2}$, $p=1,2,...,n=0,1,...,$

$$q_p=\left(\varepsilon_0\gamma_{zp}^{(2)}-\kappa_{zp}^{(2)}\right)\left(\varepsilon_0\gamma_{zp}^{(2)}+\kappa_{zp}^{(2)}\right)^{-1}, \quad (11)$$

$$\frac{\tilde{A}_m}{A_m}=J_0\left(\frac{bj_{0m}}{a}\right)\frac{j_{0m}}{a}, \quad \frac{\tilde{B}_p}{B_p}=\frac{bJ_1(j_{0p})}{2}, \quad (12)$$

$$\frac{\tilde{C}_0}{C_0}=\ln\left(\frac{a}{b}\right), \quad \frac{\tilde{C}_n}{C_n}=\frac{a^2}{2b}\frac{Z_n^2(a\chi_n)}{Z_n(b\chi_n)}-\frac{b}{2}Z_n(b\chi_n). \quad (13)$$

According to the residue-calculus technique [3, 4], in order to solve systems (7)–(9) one should construct the function $f(w)$ which satisfies the following conditions: (i) $f(w)$ is regular in complex plane w excluding first-order poles $w=\gamma_{zp}^{(3)}$; (ii) has first-order zeros for $w=\gamma_{zp}^{(1)}$ excluding $p=l$; (iii) $f(w)\xrightarrow[|w|\to\infty]{} w^{-(\tau_0+1/2)}$ with $\sin(\pi\tau_0)=(\varepsilon_0-1)/(2\varepsilon_0+2)$; (iv) $f(w)$ satisfies the relation $f(\gamma_{zn}^{(2)})+q_pf(-\gamma_{zn}^{(2)})=0$ (v) and normalized so that $f(\gamma_{zl}^{(1)})=bJ_1(j_{0p})\gamma_{zl}^{(1)}$. Asymptotic (iii) follows from Meixner's edge condition for $\rho=b$, $z\to+0$. It follows from (iii) and (iv) that $f(w)$ has first-order zeros $\Gamma_n^{(2)}=\gamma_{zn}^{(2)}+\pi/d\Delta_n^{(2)}$ shifted with respect to $\gamma_{zn}^{(2)}$. Considering integrals over circle C_∞ with infinite radius

$$\oint_{C_\infty}\frac{f(w)}{w-\gamma_{zp}^{(1)}}dw=\oint_{C_\infty}\left(\frac{f(w)}{w-\gamma_{zn}^{(2)}}+\frac{q_nf(w)}{w+\gamma_{zn}^{(2)}}\right)dw=0, \quad (14)$$

$$\oint_{C_\infty}\frac{f(w)}{w+\gamma_{zp}^{(1)}}dw=\oint_{C_\infty}\left(\frac{q_nf(w)}{w-\gamma_{zn}^{(2)}}+\frac{f(w)}{w+\gamma_{zn}^{(2)}}\right)dw=0, \quad (15)$$

we obtain $\tilde{A}_p=\mathrm{Res}\, f(\gamma_{zp}^{(3)})$, $\tilde{B}_n=-f(-\gamma_{zp}^{(1)})(2\gamma_{zp}^{(1)})^{-1}$,

$$\tilde{C}_n=\frac{\left(q_nf(\gamma_{zn}^{(2)})+f(-\gamma_{zn}^{(2)})\right)}{4\gamma_{zn}^{(2)}\kappa_{zn}^{(2)}}\left(\varepsilon_0\gamma_{zn}^{(2)}+\kappa_{zn}^{(2)}\right). \quad (16)$$

Function $f(w)$ can be constructed in the form

$$f=P_0\frac{\left(w-\Gamma_0^{(2)}\right)\prod_{n=1}^{\infty}\left(1-\frac{w}{\Gamma_n^{(2)}}\right)}{\prod_{m=1}^{\infty}\left(1-\frac{w}{\gamma_{zm}^{(3)}}\right)}\prod_{\substack{s=1,\\ s\neq l}}^{\infty}\left(1-\frac{w}{\gamma_{zs}^{(1)}}\right)G(w), \quad (17)$$

$$G(w)=\exp\left[-\frac{w}{\pi}\left(b\ln\left(\frac{b}{d}\right)+a\ln\left(\frac{d}{a}\right)\right)\right], \quad (18)$$

where $d=a-b$ and P_0 is chosen so that (v) is fulfilled. Condition (iii) dictates that $\Delta_n^{(2)}\xrightarrow[n\to\infty]{}\pi\tau_0/d$. Values $\Delta_n^{(2)}$ are obtained from (iv) using iteration process (see [4, 3, 5] for details).

In order to obtain solution for the problem (b), one should put $q_n=1$ in the condition (iv) and find the shifted zeros again. In this case $C_n=0$, and other coefficients are determined by the same formulas.

NUMERICAL CALCULATIONS AND DISCUSSION

Direct numerical simulations (using Comsol Multiphysics package) were performed in order to verify developed analytical algorithm. Moreover, in numerical simulations we consider dielectric loaded waveguides as well.

For each simulation the 3D model consists of two cylindrical "tubes" with different radii, which are connected with a flange. The length of each part is set to be ten times greater than the wavelength in the filling medium (dielectric or vacuum). The incident mode is launched and reflected/transmitted modes are received at the outer edge of each waveguide piece. Desired eigenmodes are calculated using pre-defined out-of-plane wave numbers.

Table 1: Comparison of the fractions of the transmitted W_t and reflected W_r power for the problem (b). Incident mode is TM_{01}, $\omega=2\pi\cdot 80$ GHz, $b=2.4$ mm.

Outer radius a	**Comsol** W_t	**Analytic** W_t	**Comsol** W_r	**Analytic** W_r
4.8 mm	93.0%	93.0%	7.0%	7.0%
9.6 mm	99.2%	99.2%	0.8%	0.8%
19.2 mm	96.8%	98.4%	3.2%	1.6%

Firstly, we compare numerical (Comsol) and analytical results for the problem (b). In the Table 1, we compare the ratios of the transmitted/reflected power to the power of the incident field for the launched TM_{01} mode with frequency 80 GHz and for different outer waveguide radius (small waveguide radius is b=2.4mm). Small waveguide has single propagating mode, while the larger waveguide can possess up to ten propagating modes depending on a. As one can see, results of both methods are in a good agreement. In addition, top plot of Fig. 2 represents distribution of the electric field absolute value for the case where a=2b=4.8mm.

Table 2: Comparison of the fractions of power transmitted into coaxial area (2) $W_t^{(2)}$, into vacuum area (3) $W_t^{(3)}$ and reflected power W_r for the problem (a) with $\varepsilon_0=5000$. Incident mode is TM_{01}, ω=2$\pi\cdot$ 80 GHz, b=2.4 mm.

a	$W_t^{(2)}$	$W_t^{(3)}$	W_r	Balance
4.8 mm	1.4%	91.6%	7.0%	100.0%
9.6 mm	1.0%	98.1%	0.9%	100.0%
19.2 mm	2.0%	96.8%	1.7%	100.5%

We also briefly discuss numerical results for the problem (a). It seems that for $\varepsilon_0\to\infty$ problem (a) transforms to problem (b). Strictly speaking, this is generally not the case due to certain difference in field behavior near the edge $\rho=b$, $z\to+0$ (see [4] for details). Moreover, based on the above formulas, we have developed numerical algorithm which allows calculating mode structure for arbitrary ε_0 including very large values.

ISBN 978-3-95450-181-6

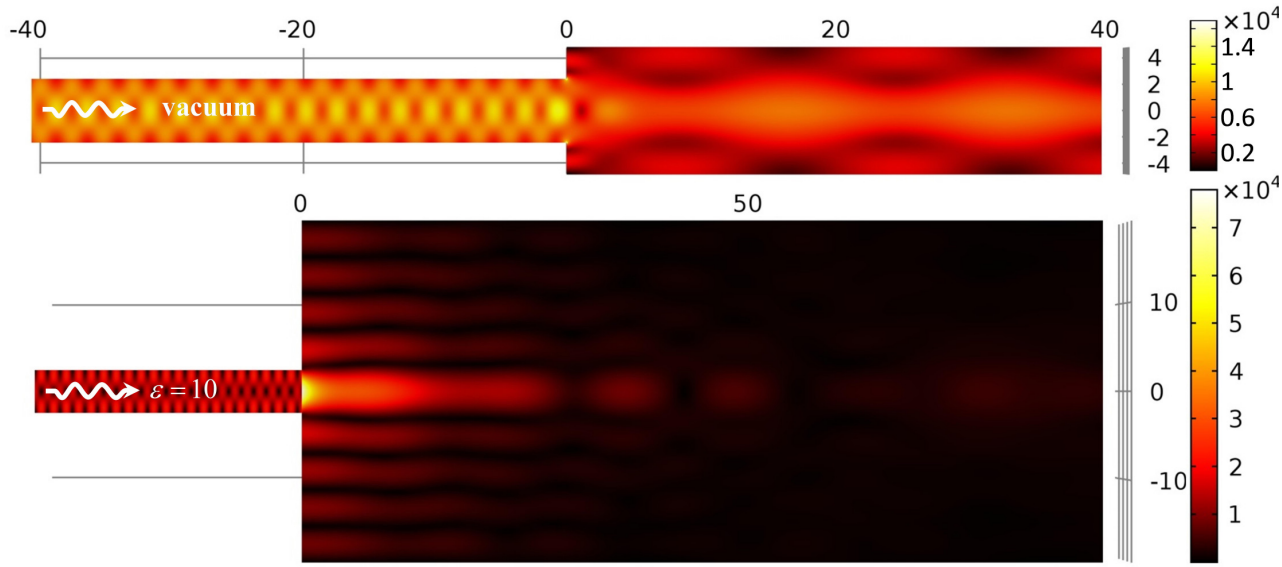

Figure 2: Distribution of the electric field absolute value for the case of the mode launching from the empty waveguide (top) and dielectric loaded waveguide (bottom), both with flanges. Structure parameters: $b = 2.4$ cm, $a = 2b$ (top), $a = 8b$, $\varepsilon = 10$ (bottom). Incident mode is TM_{01}, distances are in mm, electric field is in V/m.

Table 2 shows transmitted and reflected powers for the case (a) with $\varepsilon_0 = 5000$. Reflected power is close to that in problem (b), but power transmitted into area (3) is slightly smaller because $1-2\%$ of power goes in the coaxial waveguide despite of very high permittivity.

In numerical simulations, we also analyzed flanged waveguide with dielectric loading (problem (c)). As an example we consider material with permittivity $\varepsilon = 10$. At frequency $\omega = 2\pi \cdot 37$ GHz the dielectric waveguide has two propagating modes for $b = 2.4$ mm. In Table 3 comparison of the percentages of the reflected and transmitted power is given for different numbers of launching mode and radii a. As one can see, at a higher number of launching mode, the output power sufficiently decreases. The same situations was observed for the case of flange absence [3]. An illustration of the electric field distribution inside considered structure is given in Fig. 2, bottom row. We can see a strong evanescent field excitation near the conjunction, but the total output power is only 11% from the power of the launched mode.

CONCLUSION

We have developed rigorous theory for describing mode transformation at the discontinuity of cylindrical waveguide with dielectric layer and ideally conducting flange. For the case of vacuum flange, analytical results were in very good agreement with direct simulation using Comsol package. Moreover, analytical approach allows consideration of cases with very high permittivity (several thousands and larger). Using simulations, the case with flange and smaller radius waveguide filled with dielectric was also investigated. Compared to the case without flange, transmitted power is larger.

Table 3: Comparison of the fractions of the transmitted W_t and reflected W_r power depending on a and launching mode for problem (c); $\omega = 2\pi \cdot 37$ GHz, $b = 2.4$ mm, $\varepsilon = 10$.

Outer radius a	**Launching mode**	**Reflected power** W_r	**Transmitted power** W_t
4.8 mm	TM_{01}	82.9%	17.1%
9.6 mm	TM_{01}	85.1%	14.9%
19.2 mm	TM_{01}	89.1%	10.9%
4.8 mm	TM_{02}	99.8%	0.2%
9.6 mm	TM_{02}	99.9%	0.1%
19.2 mm	TM_{02}	99.9%	0.1%

REFERENCES

[1] S. Antipov et al., Appl. Phys. Lett. 100, 132910 (2012).

[2] S.N. Galyamin, A.V. Tyukhtin, S.S. Baturin, S. Antipov, Opt. Express 22(8), 8902 (2014).

[3] S. N. Galyamin, A. V. Tyukhtin, S. S. Baturin, V. V. Vorobev and A. A. Grigoreva, in Proc. IPAC'2016. pp. 1617-1619.

[4] R. Mittra and S. W. Lee, *Analytical techniques in the theory of guided waves* (Macmillan, 1971).

[5] S.N. Galyamin, A.V. Tyukhtin, A.M. Altmark, S.S. Baturin, WEPSB069, these proceedings.

ISBN 978-3-95450-181-6